Model assumptions in Coulex analysis and other GOSIA tricks

Magda Zielińska
IRFU/SPhN, CEA Saclay

- Model assumptions for a well-deformed odd-A case: ^{97,99}Rb
- Efficiency of particle detectors
- Optimal subdivision of Coulex data

Coulomb excitation of $^{97-99}$Rb at ISOLDE

- identification of rotational bands in $^{97-99}$Rb (first observation of collective states in these nuclei!)
- statistics sufficient for gamma-gamma coincidences – level schemes established

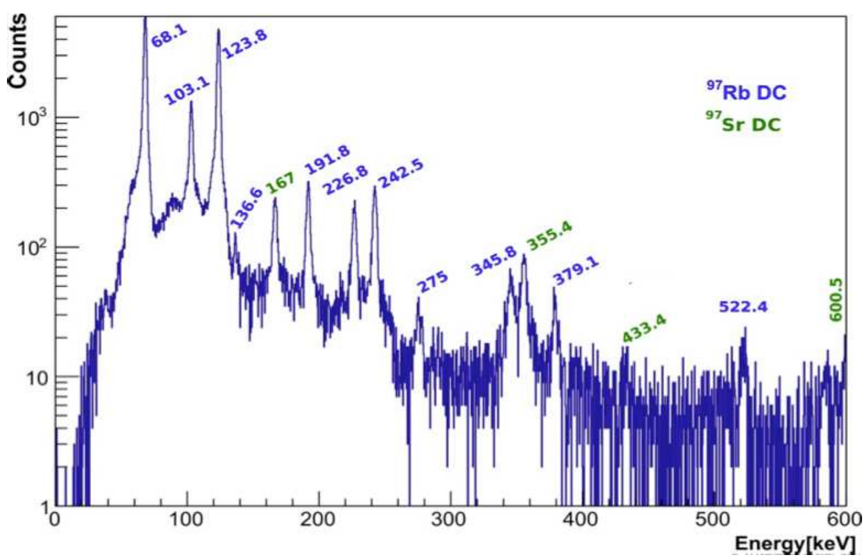

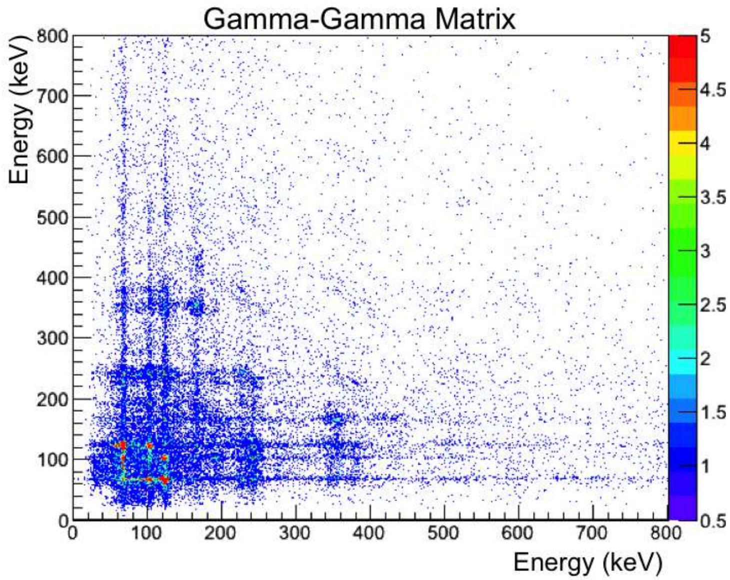

Ch. Sotty, Phys. Rev. Lett. 115 (2015) 172501

- Second step: extraction of E2 and M1 matrix elements using GOSIA code

Problems in Coulex data analysis (^{97}Rb)

- Cline's safe Coulex criterion not fulfilled for high CM angles
- efficiency for the 68 keV line uncertain
- 355 keV transition obscured by a line in ^{97}Sr
- underdetermined problem: 20 gamma rays, 24 matrix elements (E2 and M1)
- very strong correlations between matrix elements

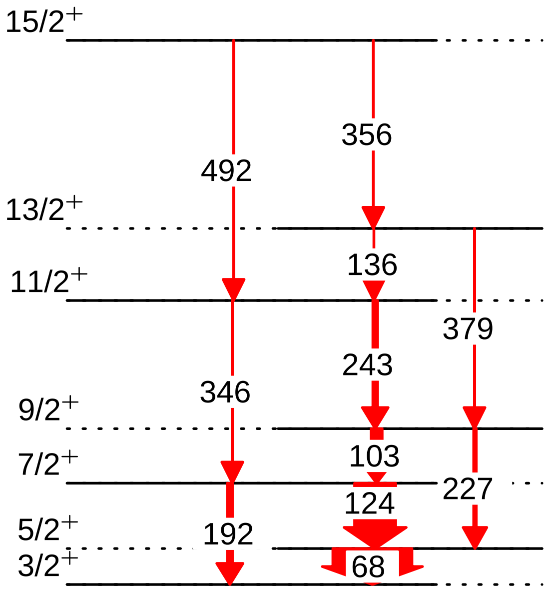

Problems in Coulex data analysis (^{97}Rb) and solutions

- Cline's safe Coulex criterion not fulfilled for high CM angles

→ 15 % of statistics excluded from the analysis

- efficiency for the 68 keV line uncertain

→ would be a natural choice for normalisation but had to be excluded from the analysis

- 355 keV transition obscured by a line in ^{97}Sr

→ intensity obtained from gamma-gamma coincidences

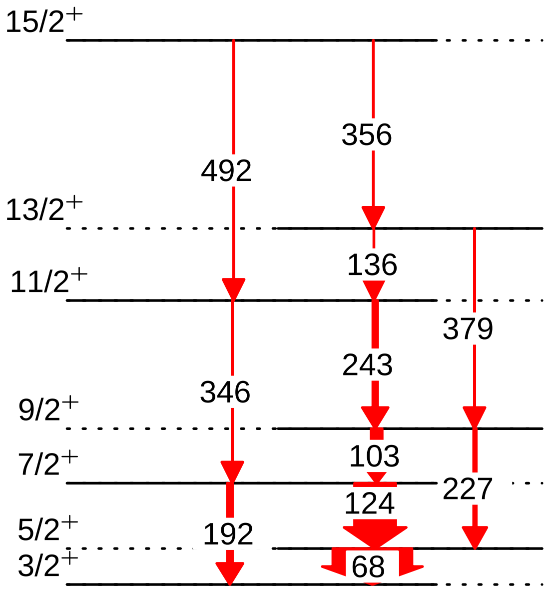

- underdetermined problem: 20 gamma rays, 24 matrix elements (E2 and M1)

→ model assumptions necessary: Alaga rules

$$\langle KI_f || E2 || KI_i \rangle = \sqrt{(2I_i + 1)} (I_i, K, 2, 0 | I_f, K) \sqrt{\frac{5}{16\pi}} eQ_0$$

⇒ within rotational model E2 branching ratio depends on spins only (Q_0 cancel out)

- very strong correlations between matrix elements

→ large uncertainties for low-lying transitions

Normalisation to target excitation

- for each value of $\langle 7/2^+ \| E2 \| 3/2^+ \rangle$ all remaining matrix elements in Rb and Ni are fitted to observed gamma-ray intensities and known spectroscopic data (GOSIA2)
- Alaga rules assumed for each pair of I $\rightarrow$ I-1 and I $\rightarrow$ I-2 E2 transitions

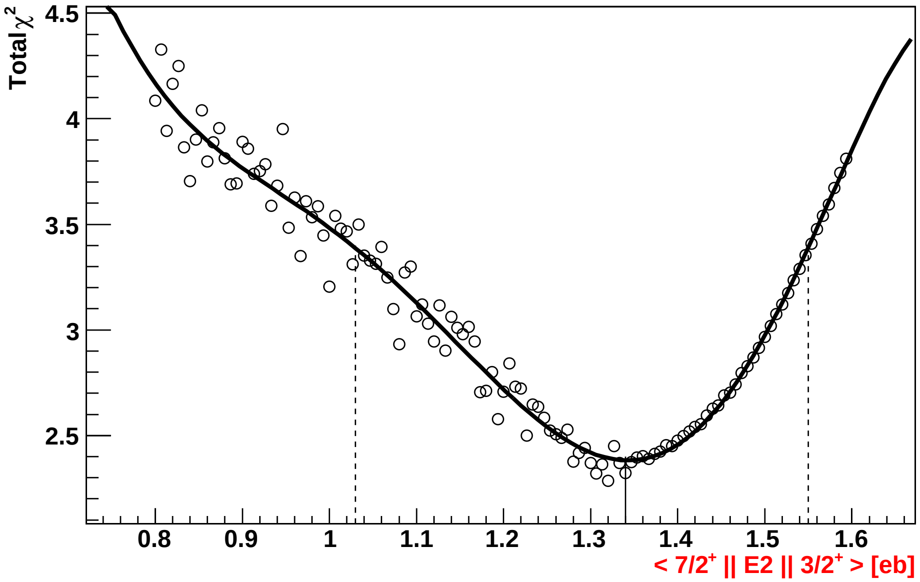

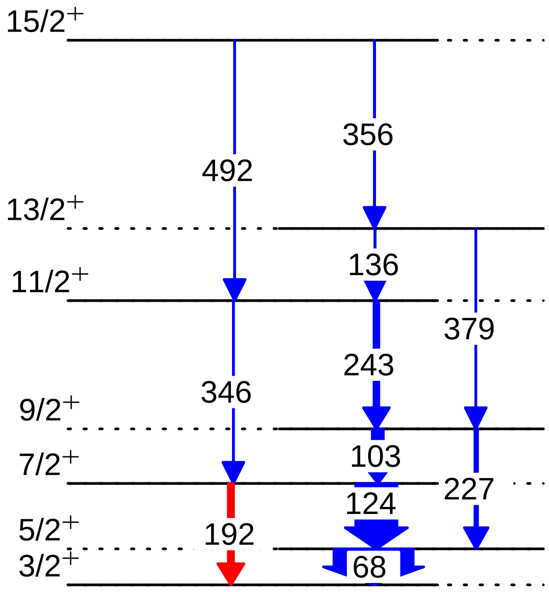

- for all other transitions a standard GOSIA1 analysis assuming this value of $\langle 7/2^+ \| E2 \| 3/2^+ \rangle$

Normalisation to target excitation

Convergence problems

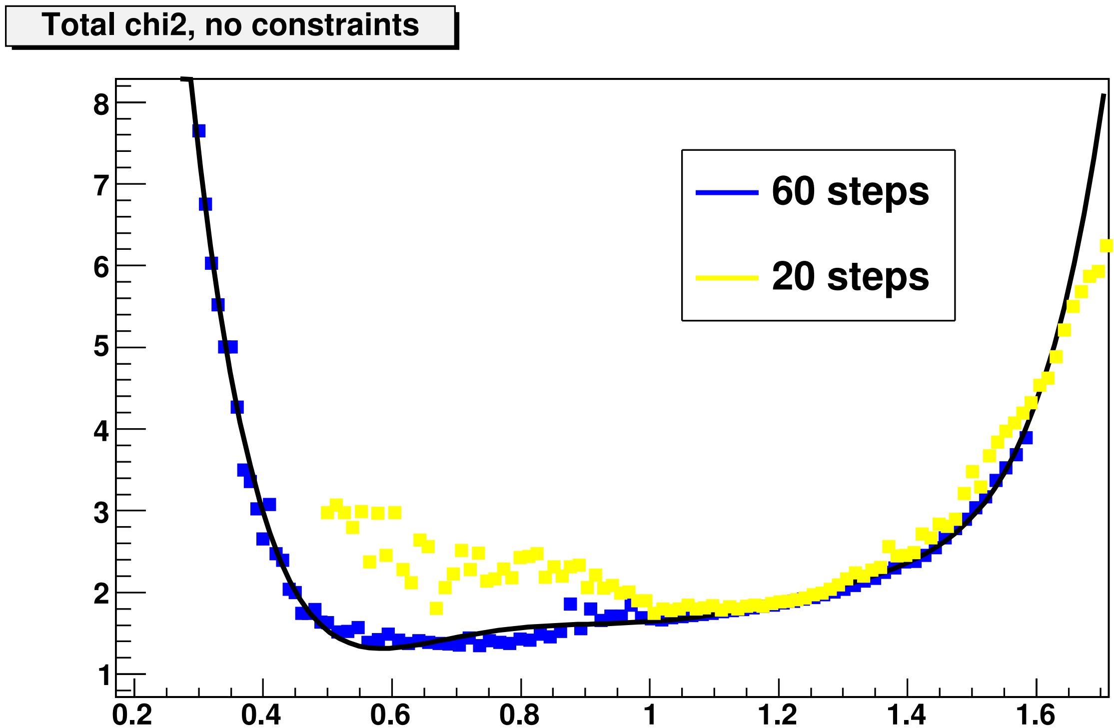

- fluctuations due to a local χ^2 minimum, more iterations give a more smooth dependence (and a new global minimum)
- smooth parts of the χ^2 curve don't change much

Normalisation to target excitation

Different minimum if E2 branching ratios imposed

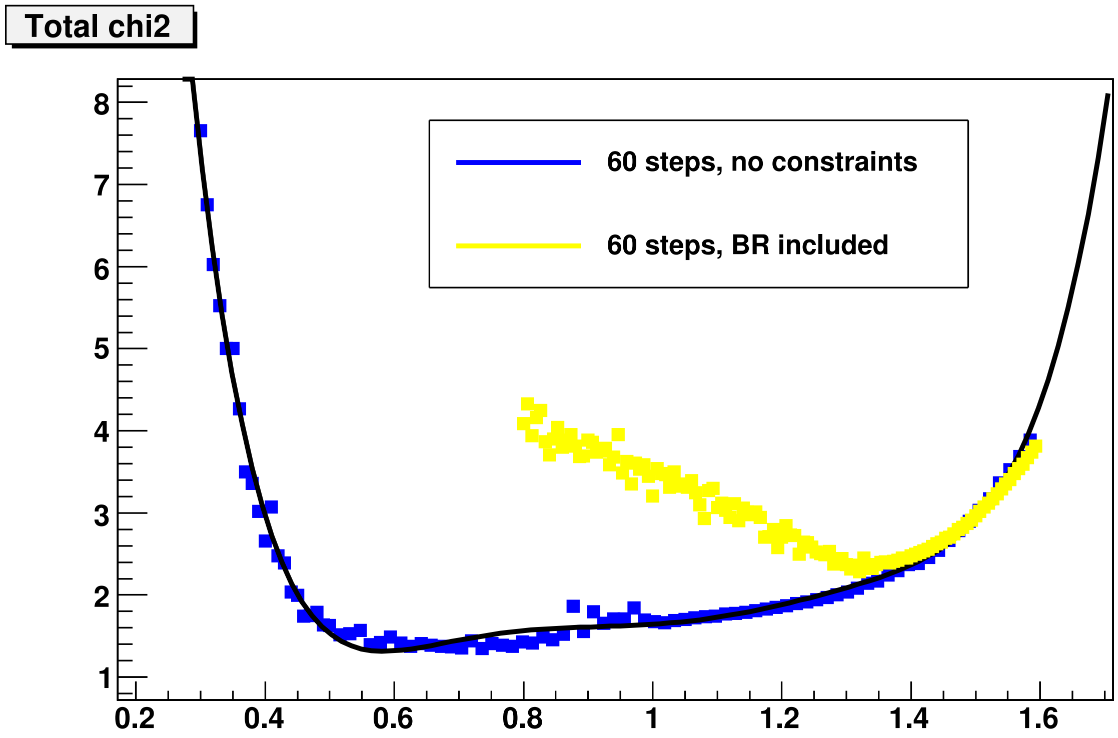

Results: deformation of ^{97}Rb

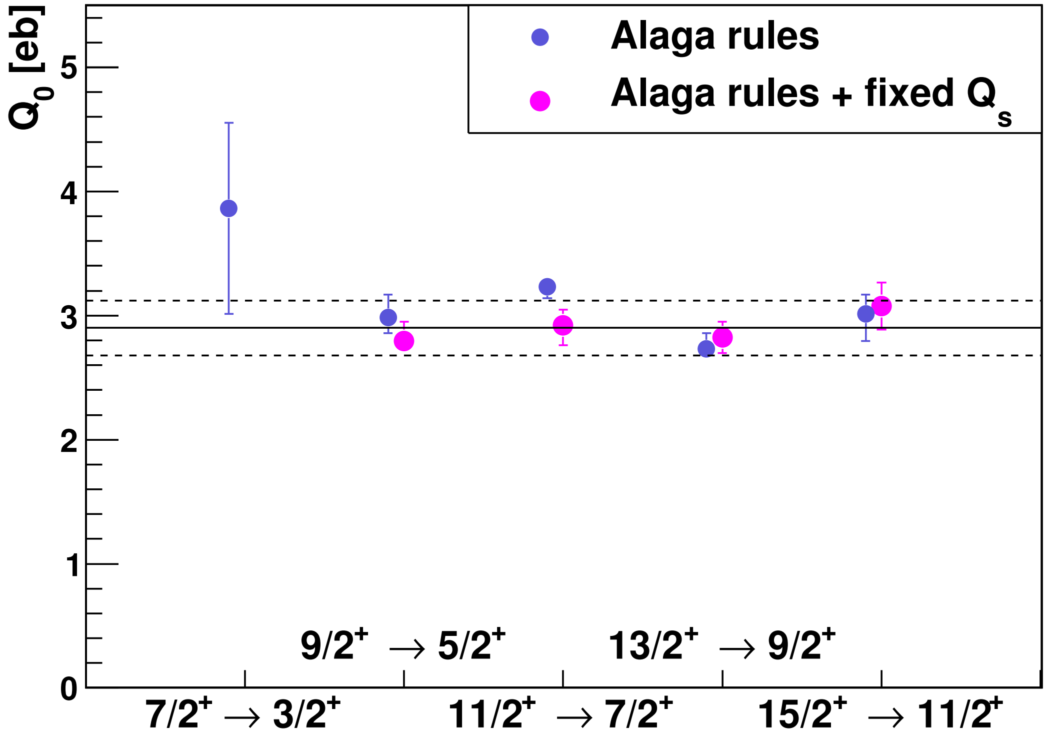

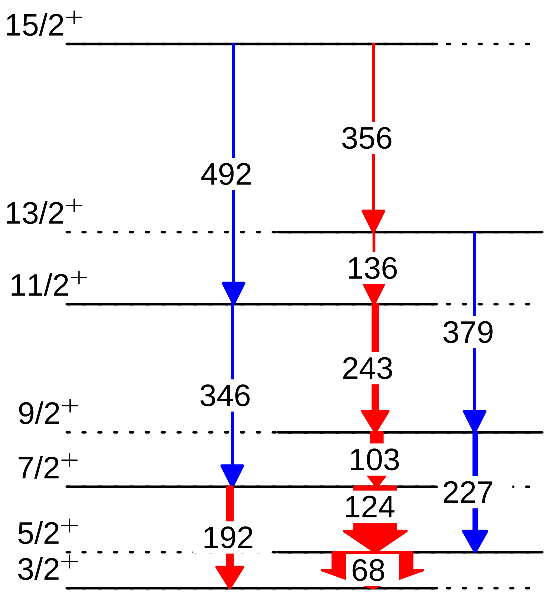

- two different assumptions give consistent results for 4 matrix elements
- these 4 transitions are populated in multi-step excitation → matrix elements related to observed intensity ratios in ^{97}Rb (no need for other normalisation)
- results consistent with Q_{sp} of the g.s. measured in laser spectroscopy (horizontal lines)

Next step: ^{99}Rb

Problems we know already from ^{97}Rb:

- Cline's safe Coulex criterion not fulfilled for high CM angles
- efficiency for the 65 keV line uncertain
- very strong correlations between matrix elements

New problems:

- very low statistics (few hundred counts in the strongest line)
- target excitation not observed
- unresolved doublet at 222 keV
- extremely underdetermined problem: 6 gamma rays, 15 matrix elements)

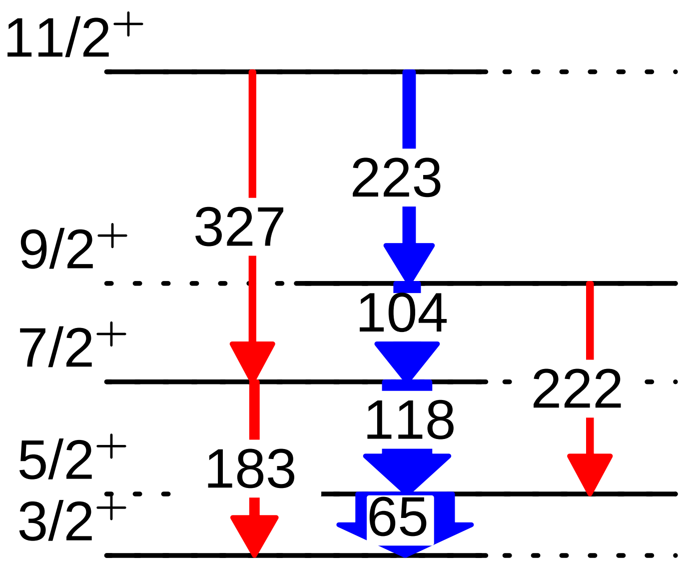

^{99}Rb: proposed solution and test on ^{97}Rb data

- matrix elements in the upper part of a strongly deformed rotational band related to observed intensity ratios in the nucleus under study (no external normalisation required)
- all E2 matrix elements (including Q_s) coupled using rotational model
- then we fit only M1 matrix elements and one Q_0 to measured gamma-ray intensities
- tested on ^{97}Rb data, result consistent with weighted average of Q_0 values obtained in standard analysis

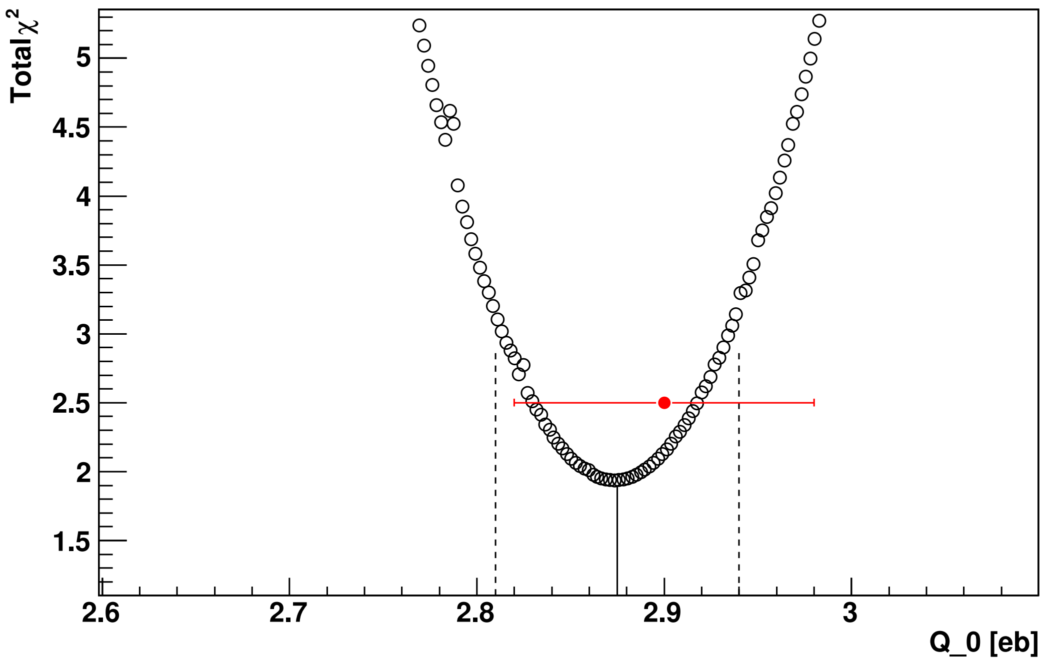

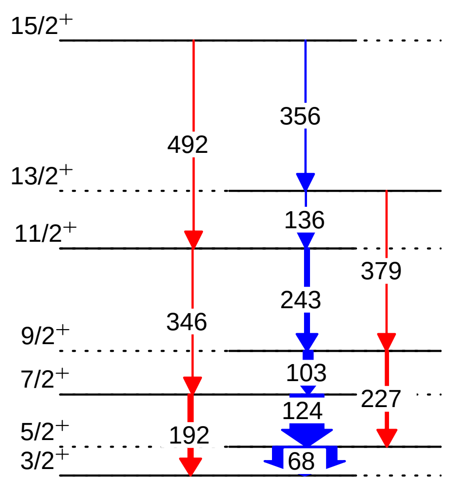

^{99}Rb: results

- 4 M1 matrix elements and one Q_0 fitted to measured gamma-ray intensities in ^{99}Rb

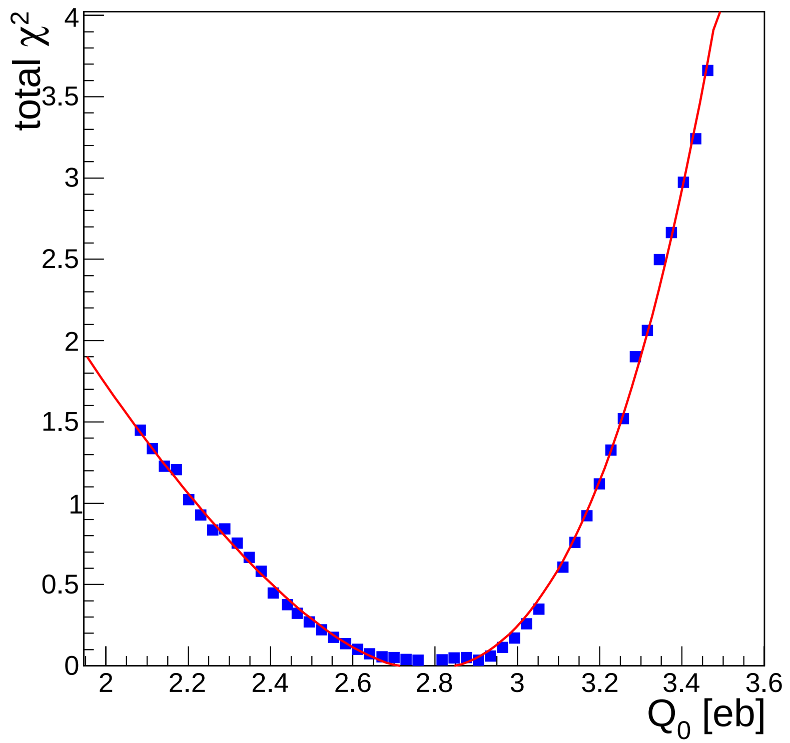

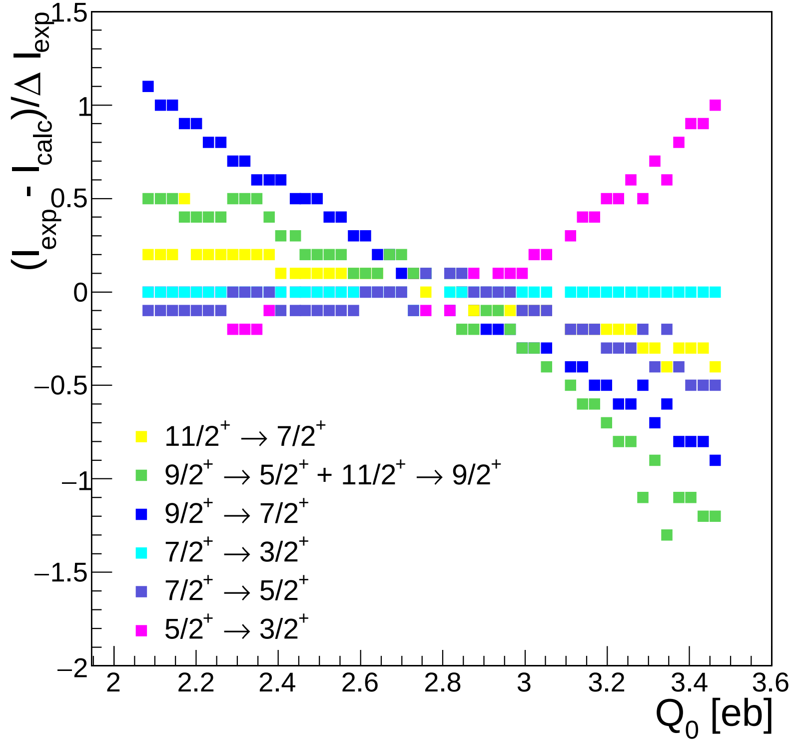

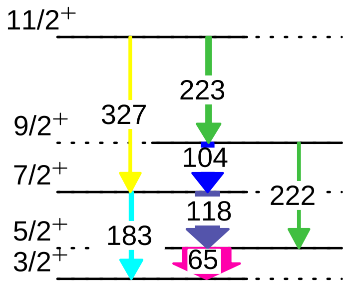

- one clear χ^2 minimum for all observed transitions
- precision rather low due to limited statistics

Deformation of ^{99}Rb: comparison with ^{97}Rb

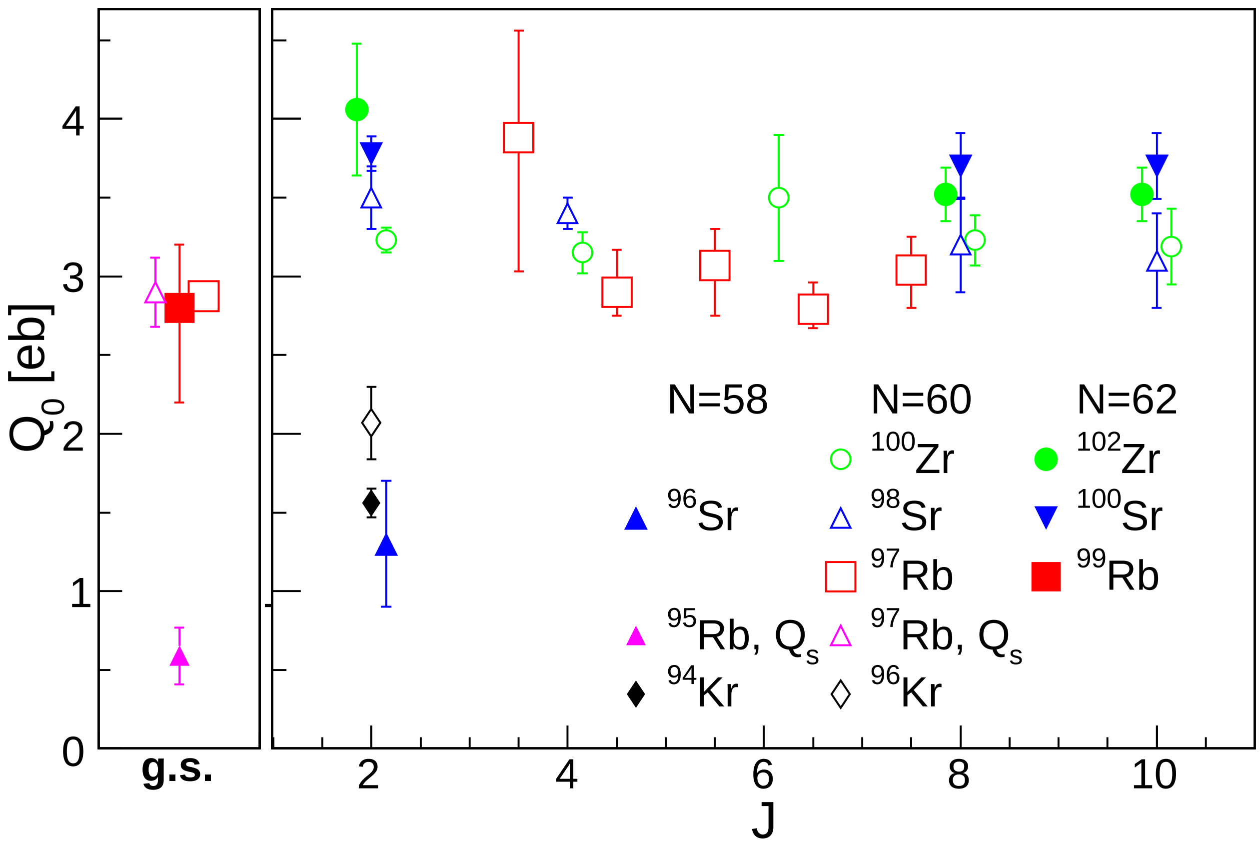

Efficiency of particle detectors

two ways to account for it

Efficiency of a particle detector

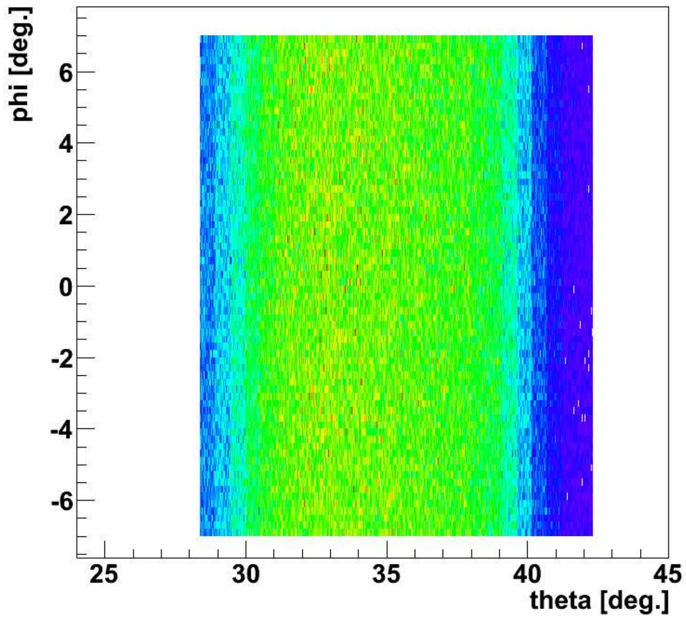

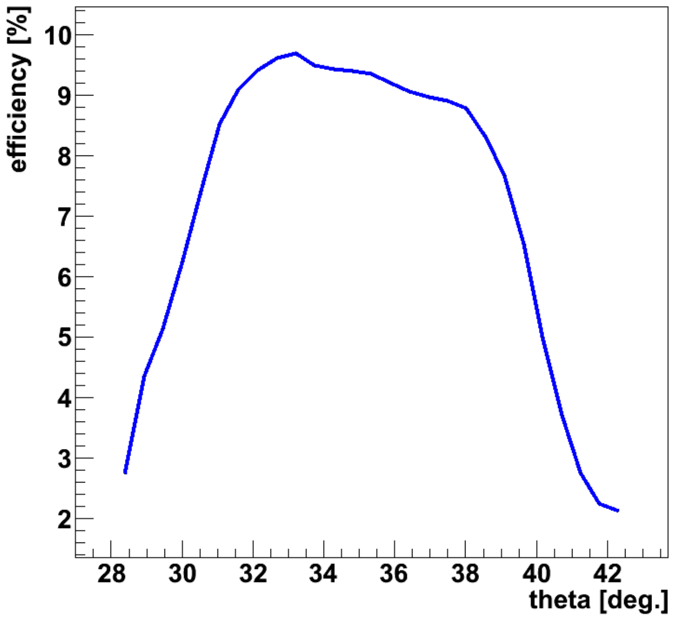

- efficiency doesn’t have to be uniform for all the detector’s area
- some parts of the detectors can stop working at some point
- if the detector has a uniform efficiency lower than 100% it’s fine (it’s included in the normalisation constant of the experiment)

Efficiency of a particle detector

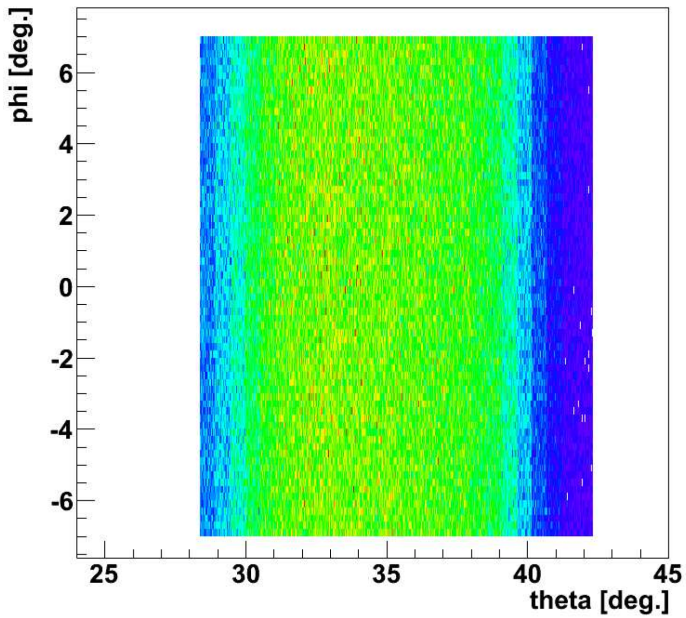

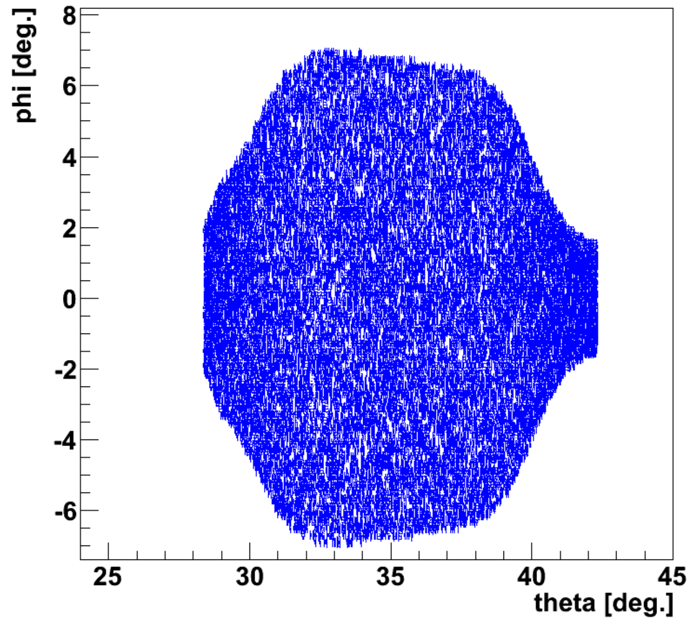

Solution 1:

- Coulomb excitation strength depends on θ scattering angle – one can modify detector shape in φ to take the efficiency into account
- applicable if we have a symmetric gamma detection set-up (gamma-particle correlations smoothed out)
- φ range covered by the detector scaled according to efficiency: true range (here: (-7°,7°)) where efficiency is maximal, reduced to (-3.5°,3.5°) where it's only 50% of the maximum value, etc.

Efficiency of the particle detector: second solution

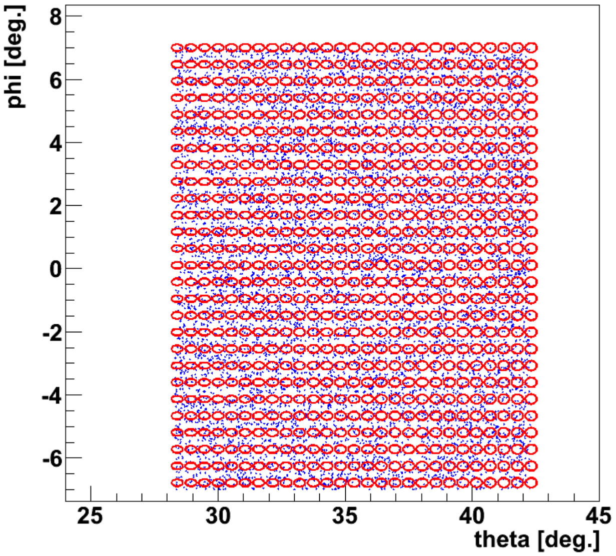

OP,INTG
3, 3, 683.2, 690.7, 28.38, -6.62, 0.223
683.2, 687, 690.7
3, 3, ...
...

- detector shape approximated by a large number (here: 729) of small circular detectors
- first step: comparison with a 100% efficiency detector, angular range covered by a single detector chosen to reproduce the Rutherford cross section

Efficiency of the particle detector: second solution

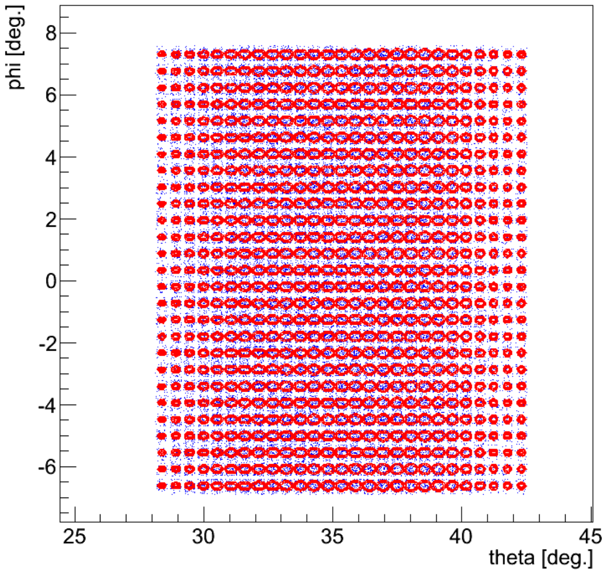

OP,INTG
3, 3, 683.2, 690.7, 28.38, -6.62, 0.119
683.2, 687, 690.7
3, 3, ...
...

- detector shape approximated by a large number (here: 729) of small circular detectors
- first step: comparison with a 100% efficiency detector, angular range covered by a single detector chosen to reproduce the Rutherford cross section
- second step: detector areas scaled according to efficiency (θ_{half} scaled as $\sqrt{A}$)
- does not change the φ coverage of the detector – better if particle-gamma correlations important

Comparison of results

Integrated yields, normalised to $2_1^+ \to 0_1^+$ (YCOR)

transition	eff vs standard	PIN vs standard	PIN, eff vs PIN
$14_1^+ \to 12_1^+$	18.5%	-2.8%	19.3%
$12_1^+ \to 10_1^+$	13.6%	-2.0%	13.6%
$10_1^+ \to 8_1^+$	8.2%	-1.0%	7.8%
$6_2^+ \to 6_1^+$	4.3%	-0.4%	3.5%
$8_1^+ \to 6_1^+$	0.7%	0.0%	0.0%
$4_2^+ \to 4_1^+$	-3.4%	0.7%	-4.0%
$2_2^+ \to 2_1^+$	-1.2%	0.0%	-1.2%
$6_1^+ \to 4_1^+$	-1.7%	0.7%	-2.7%
$4_1^+ \to 2_1^+$	-1.1%	0.5%	-1.6%
$2_1^+ \to 0_1^+$	0.0%	0.0%	0.0%
Rutherford	-23.2%	0.5%	-25.7%

- both solutions work reasonably well
- corrections important for multi-step and non-yrast states

Buffer states

Buffer states

- reorientation effect can be comparable with population of higher-lying states
- when analysing Coulex data, we should include buffer states on top of bands to account for possible excitation of higher-lying states
- otherwise we get incorrect quadrupole moments
- rotational model can be used to estimate starting values of ME

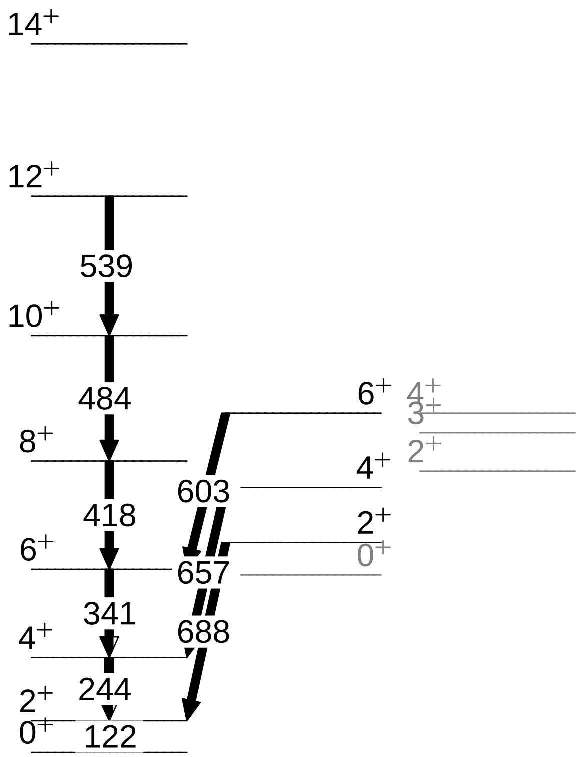

Optimal subdivision of Coulex data

Where is sensitivity to quadrupole moments coming from?

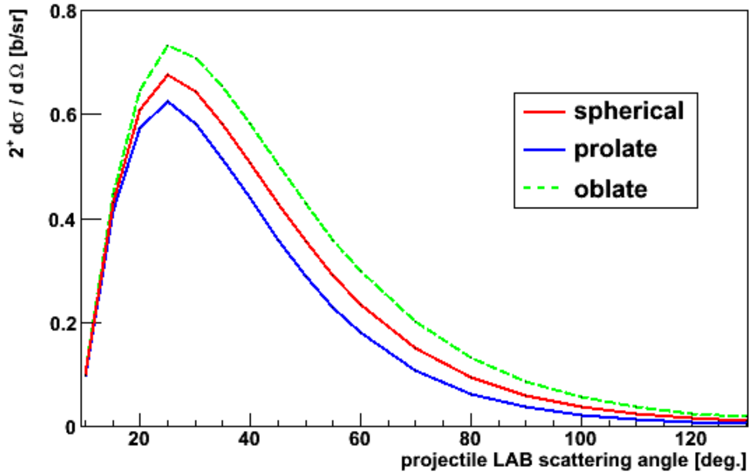

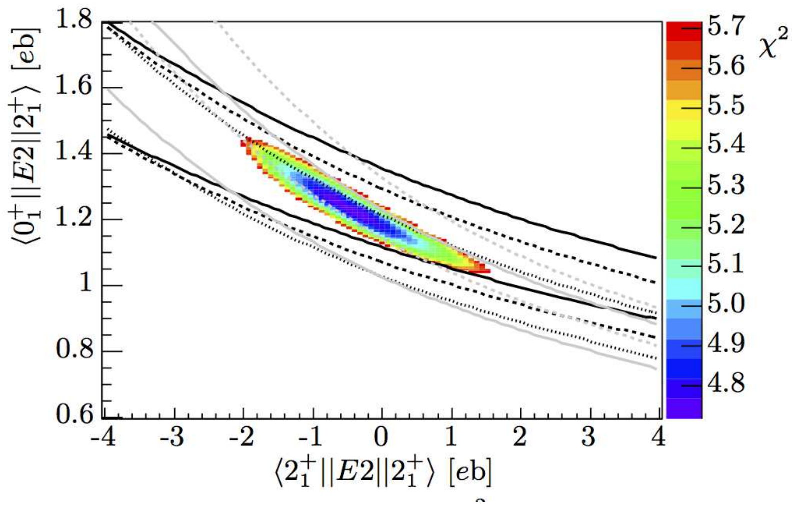

L. Gaffney et al., Phys. Rev. C 91, 064313 (2015)

- compromise between number of subdivisions and statistics
- useful to have a range where the influence of $\langle 2^+ \| E2 \| 2^+ \rangle$ is negligible (horizontal cut), but not always possible
- for high CM angles influence of quadrupole moment should be higher than statistical error of the gamma yield
- if two cuts in $\langle 2^+ \| E2 \| 2^+ \rangle$, $\langle 2^+ \| E2 \| 0^+ \rangle$ plane are really close, probably you will gain more by combining the statistics

Backup slides: how to describe complicated detector shapes in GOSIA

(step by step!)

Efficiency included by modifying the detector shape

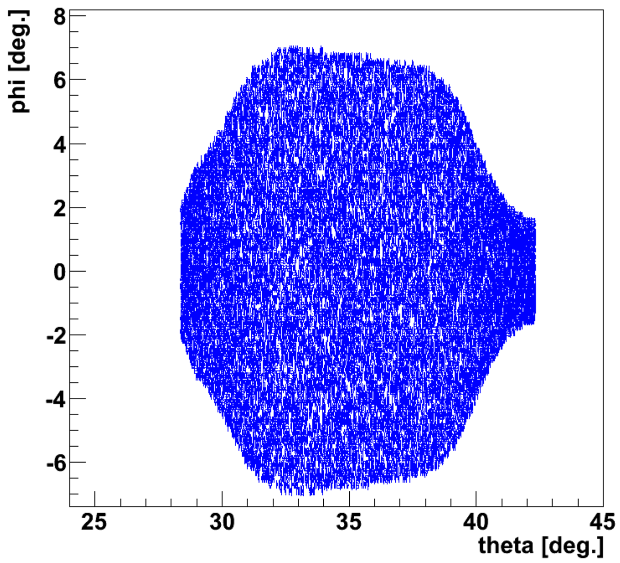

OP,INTG
3,

- number of energy meshpoints

Efficiency included by modifying the detector shape

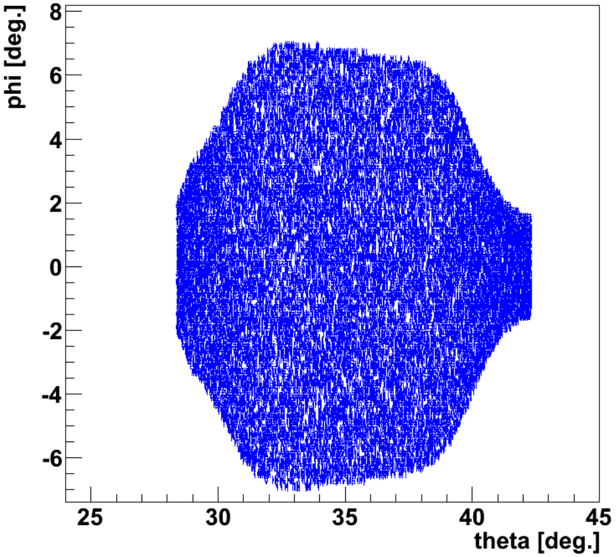

OP,INTG
3,-13,

- number of energy meshpoints
- number of θ meshpoints (with „-” sign if we plan to introduce the $\varphi(\theta)$ dependence)

Efficiency included by modifying the detector shape

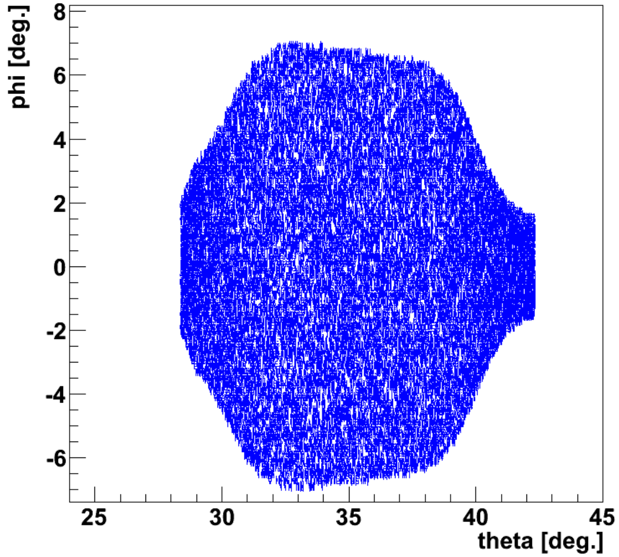

OP,INTG
3,-13,683.2,690.7,

- number of energy meshpoints
- number of θ meshpoints (with „-” sign if we plan to introduce the $\varphi(\theta)$ dependence)
- minimum and maximum bombarding energy

Efficiency included by modifying the detector shape

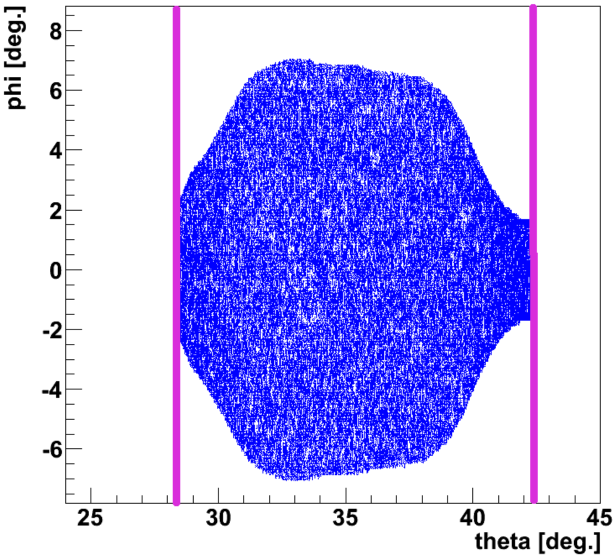

OP,INTG
3,-13,683.2,690.7,28.3,42.3,

- number of energy meshpoints
- number of θ meshpoints (with „-” sign if we plan to introduce the $\varphi(\theta)$ dependence)
- minimum and maximum bombarding energy
- minimum and maximum θ angles

Efficiency included by modifying the detector shape

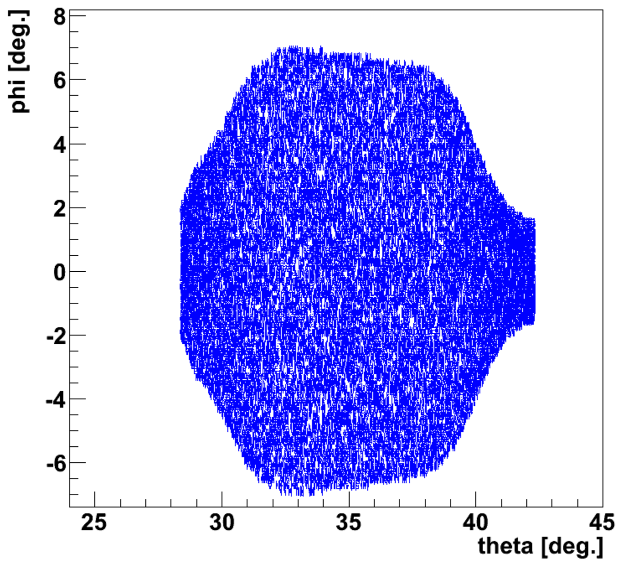

OP,INTG
3,-13,683.2,690.7,28.3,42.3,
683.2,687,690.7

- number of energy meshpoints
- number of θ meshpoints (with „-” sign if we plan to introduce the $\varphi(\theta)$ dependence)
- minimum and maximum bombarding energy
- minimum and maximum θ angles
- energy meshpoints

Efficiency included by modifying the detector shape

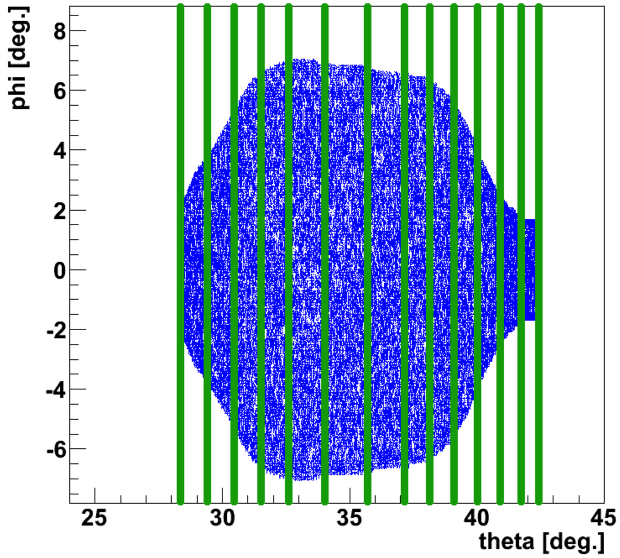

OP,INTG
3,-13,683.2,690.7,28.3,42.3,
683.2,687,690.7
28.3,29.3,30.3,31.5,33.,35,36.5,38.5,39.5,40.5,
41.5,42,42.3

- number of energy meshpoints
- number of θ meshpoints (with „-” sign if we plan to introduce the $\varphi(\theta)$ dependence)
- minimum and maximum bombarding energy
- minimum and maximum θ angles
- energy meshpoints
- theta meshpoints: among them minimum and maximum θ angles, more points where the shape is more complicated

Detector shape – continued

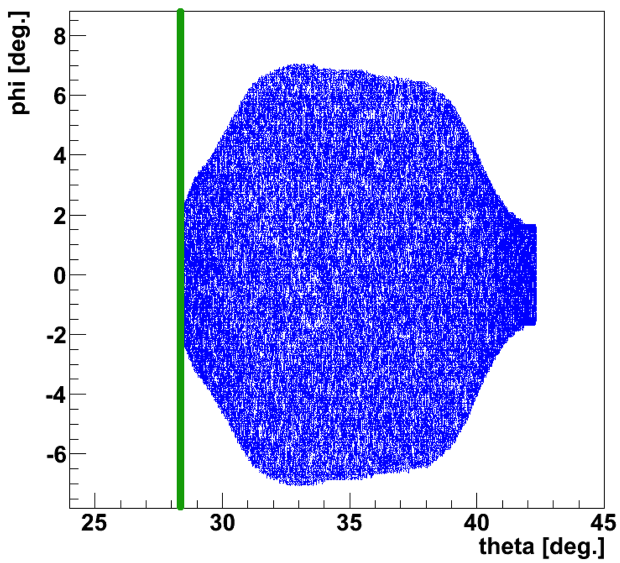

OP,INTG
3,-13,683.2,690.7,28.3,42.3,
683.2,687,690.7
28.3,29.3,30.3,31.5,33.,35,36.5,38.5,39.5,40.5,
41.5,42,42.3
1
-2,2

Then for each of the theta meshpoints we have to give the $\varphi_{minimum}$ and $\varphi_{maximum}$; if there is more than one phi range for this θ, we have to specify more such ϕ pairs.

- first point (θ = 28.3°) – one φ range (-2°, +2°)

Detector shape – continued

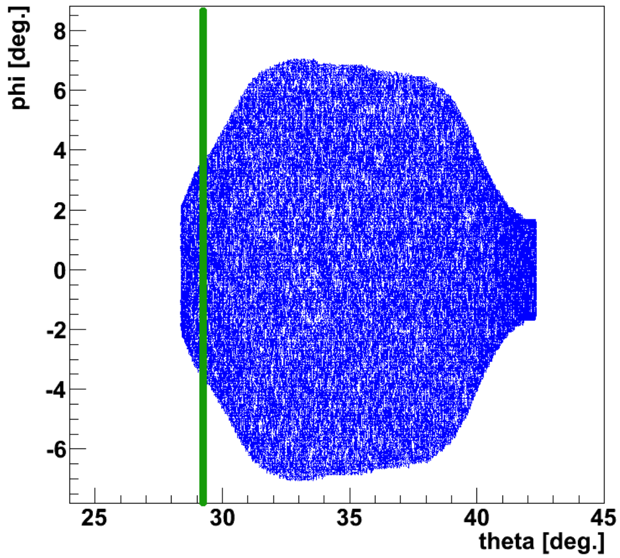

OP,INTG
3,-13,683.2,690.7,28.3,42.3,
683.2,687,690.7
28.3,29.3,30.3,31.5,33.,35,36.5,38.5,39.5,40.5,
41.5,42,42.3
1
-2,2
1
-3.6,3.6

Then for each of the theta meshpoints we have to give the $\varphi_{minimum}$ and $\varphi_{maximum}$; if there is more than one phi range for this θ, we have to specify more such ϕ pairs.

- first point (θ = 29.3°) – one φ range (-2°, +2°)
- second point (θ = 28.3°) – one φ range (-3.6°, +3.6°)
- and so on...

Detector shape – continued

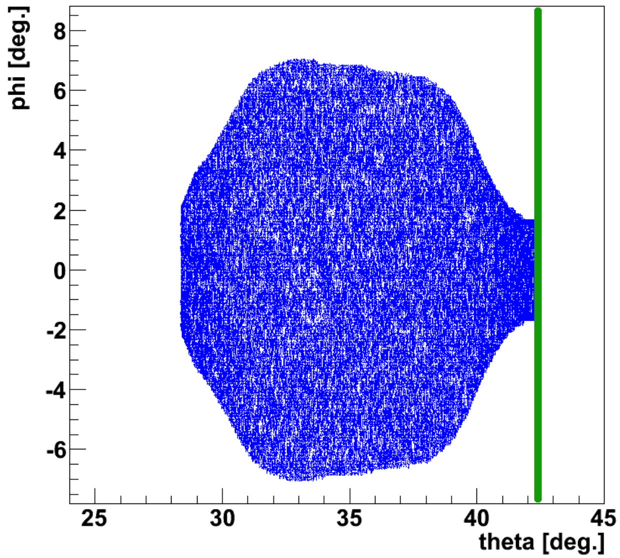

1,
-1.5, 1.5

- ...
- last point (θ = 42.3°) – one φ range: (-1.5°,1.5°)

Detector shape – continued

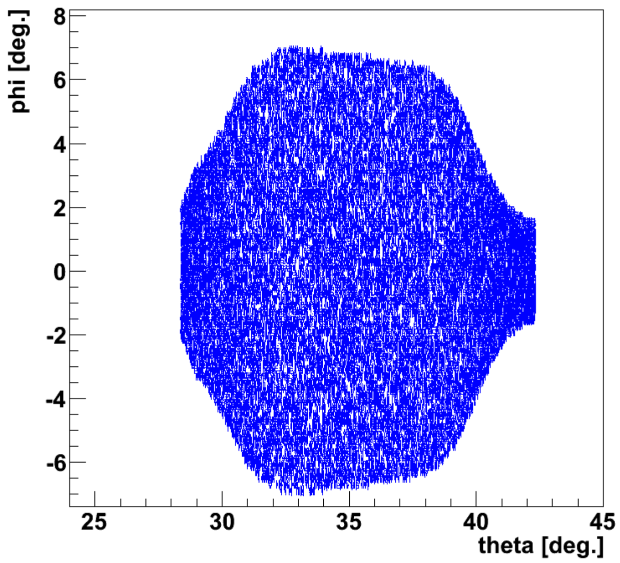

1
-1.5,1.5
3
683.2,687,690.7
30.3,30.1,29.9

Input of stopping powers:

- number of meshpoints
- energy meshpoints
- stopping powers

Detector shape – continued

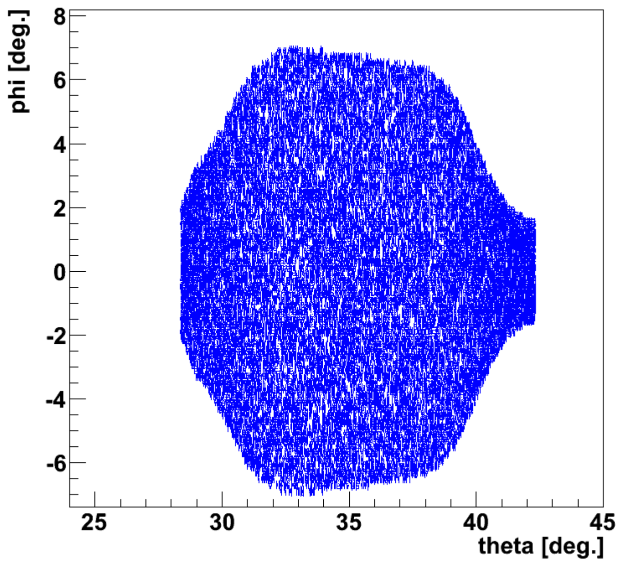

3
683.2,687,690.7
30.3,30.1,29.9
10,

- stopping powers
- number of subdivisions of energy used for interpolation (even number, maximum value 100)

Detector shape – continued

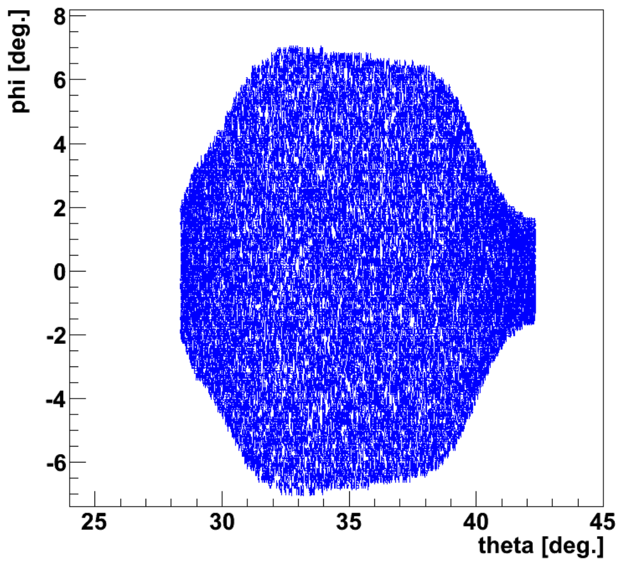

3
683.2,687,690.7
30.3,30.1,29.9
10,-26

- stopping powers
- number of equal subdivisions of energy used for interpolation (even number, maximum value 100)
- number of equal subdivisions of theta used for interpolation (even number, maximum value 100, with „-" sign if we introduce the $\varphi(\theta)$ dependence). Here: twenty six ranges, 0.8 degree each.

Detector shape – continued

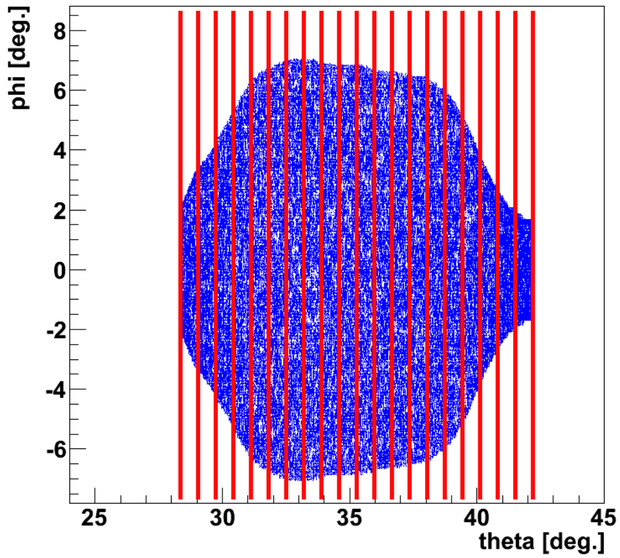

3
683.2,687,690.7
30.3,30.1,29.9
10,-26
4.0,6.3,7.4,9.0,10.7,12.3,13.1,13.6,13.9,14.0,
13.7,13.6,13.6,13.5,13.3,13.1,12.9,12.8,12.7,
12.0,11.1,9.4,7.2,5.3,4.0,3.3,3.0

- stopping powers
- number of equal subdivisions of energy used for interpolation (even number, maximum value 100)
- number of equal subdivisions of theta used for interpolation (even number, maximum value 100, with „-” sign if we introduce the $\varphi(\theta)$ dependence). Here: twenty six ranges, 0.8 degree each.
- total phi range for each cut (twenty seven points)